

The Feasibility of the First Utility-Scale Wind Farm in Saudi Arabia (The 400 MW Dumat Al-Jandal Project)

Kamel Almutairi and Ramzi Alahmadi

Abstract—Saudi Arabia has an ambitious plan to diversify its power generation resources. Part of this plan includes launching the King Salman Renewable Energy Initiative (KSREI). The goal of this work is to study the feasibility of the first utility-scale wind farm in Saudi Arabia, known as the 400 MW Dumat Al-Jandal project, and was conducted using the System Advisor Model (SAM) software. As the hub height of the wind turbine is usually different from the height at which the wind measurements are taken, the wind speeds were extrapolated to different heights using different methods. These methods are the power law using two different shear coefficients and the logarithmic law. The simulations were performed for 113 commercial wind turbines with different sizes and power curves to help enhance our understanding of the effects of these factors on wind farm performance. The technical analysis shows that the capacity factors of the most efficient wind machine types varied from 35.5%–26.8%, 32.9%–25.5%, and 29.7%–23.7% for the heights 140 m, 110 m, and 80 m, respectively. From an economic perspective, the levelized cost of energy (LCOE) of the most efficient wind machine types varied from 3.23–4.57 ¢/kWh, 3.55–4.84 ¢/kWh, and 4.02–5.82 ¢/kWh for the heights 140 m, 110 m, and 80 m, respectively. The lowest possible LCOE (3.23 ¢/kWh), according to this analysis, is in the same range of the submitted LCOE by the project’s winning bidder. Finally, the net present value (NPV) shows that the project is economically feasible.

Index Terms—Wind energy, Saudi vision 2030, System Advisor Model (SAM), levelized cost of energy (LCOE).

I. INTRODUCTION

Even though Saudi Arabia ranks second worldwide when it comes to the amount of proven crude oil reserves [1], the country has a plan, in its ambitious 2030 vision, to diversify its power generation resources. This plan is motivated by a number of factors. First, the country has impressive natural resources for harnessing different types of renewable energy, especially wind and solar energy. Second, the local energy consumption is expected to increase threefold by 2030 [2]. The current state of power generation is heavily dependent on petroleum products. In 2019 (the year of the latest published report), electricity generation by fuel type was as follows: crude oil 21.5%, gas 43.1%, heavy fuel oil 27.5%, and diesel 7.9% [3]. Saudi Arabia domestically burns more than 15% of its oil production and 50% of its gas production to generate electricity, and its domestic oil consumption is expected to reach 8.3 million barrels per day by 2028 if it continues to exhibit this pattern [4]. This massive domestic consumption

will have an effect on Saudi Arabia’s ability to export oil, which will, consequentially, result in a cut for the country’s main source of revenue: oil [5].

In addition to the economic impacts, the environment and public health are impacted by burning fossil fuels that are largely responsible for emitting the greenhouse gases causing global climate change [6]. Based on the Global Carbon Atlas, in 2019, Saudi Arabia was ranked as the 10th largest CO₂ emitter in the world, and the 10th largest in terms of CO₂ emissions per capita, as shown in Tables I and II, respectively [7].

Saudi Arabia is committed to reducing these emissions and complying with the Paris Agreement [8]. Therefore, the Saudi Arabian government launched the King Salman Renewable Energy Initiative (KSREI) that set a target of generating 58.7 GW of renewable energy by 2030. The KSREI recommends that, by 2030, Saudi Arabia’s renewable energy mix be the following: 40 GW from solar photovoltaic energy, 16 GW from wind energy, and 2.7 GW from concentrated solar power (CSP) [9]. Saudi Arabia’s Ministry of Energy established the National Renewable Energy Program (NREP), which falls under Vision 2030 and KSREI and aims to increase the renewable energy share in Saudi Arabia’s electricity mix. This renewable energy penetration will take place by encouraging a partnership between the public sector and private parties, setting guidelines and policies to create a Saudi local based renewable energy technology hub, and contributing to the energy transition and environmental commitments of the country [10].

In 2019, the NREP awarded the 400 MW Dumat Al-Jandal project to a consortium consisting of the French company EDF Renewable and the United Arab Emirates company Masdar. The Dumat Al-Jandal project, in the northern Al Jouf region, is Saudi Arabia’s first utility-scale wind farm [11]. The \$500 million project is expected to provide up to 70,000 households with power and create about 950 jobs between the construction and operation phases [10]. The winning bid’s levelized cost of energy (LCOE) for the project was 2.13–3.39 cent/kWh [11]. The project is expected to offset 994,000 tons of CO₂ annually and displace 894,000 barrels of oil equivalent per year [10]. It is expected to be completed in 2022 [12].

TABLE I: LARGEST CO₂ EMITTERS IN THE WORLD

Rank	Country	MtCO ₂
1	China	10,175
2	United States of America	5,282
3	India	2,661
4	Russian Federation	1,678
5	Japan	1,107

Manuscript received October 24, 2021; revised January 22, 2022.

Kamel Almutairi is with Chemical Engineering Department at Taibah University, Madinah, Saudi Arabia (e-mail: kmutairi@taibahu.edu.sa, almutairikamel@gmail.com).

Ramzi Alahmadi is with Industrial Engineering Department at Taibah University, Madinah, Saudi Arabia (e-mail: rlahmadi@taibahu.edu.sa).

6	Iran	780
7	Germany	702
8	South Korea	611
9	Indonesia	618
10	Saudi Arabia	582

TABLE II: LARGEST CO₂ EMITTERS IN TERMS OF CO₂ EMISSIONS PER CAPITA

Rank	Country	tCO ₂ /person
1	Qatar	39
2	Curaçao	32
3	New Caledonia	30
4	Trinidad & Tobago	27
5	Kuwait	26
6	Bahrain	21
7	Brunei	21
8	United Arab Emirates	20
9	Mongolia	20
10	Saudi Arabia	17

The ability of assessing and characterizing the availability of wind resources is a crucial factor in developing a new wind energy project. In the wind power field, it is known that a 2% error in the estimated power is the result of a 1% error in the measurement of wind speed [13]. Therefore, precise on-site wind speed measurements reduce the risk of making a wrong investment. In addition, as wind speed measurements are usually taken at heights different from the wind machine's hub height, a number of ways are used to estimate the vertical wind speed profile. The first method includes extrapolating the measured wind speed to a hub height using a coefficient called wind shear. The wind shear coefficient can be estimated by measuring the wind speed at least two heights for at least a one-year period. The wind shear coefficient α can then be calculated using the following equation:

$$\alpha = \frac{\ln(V_2) - \ln(V_1)}{\ln(Z_2) - \ln(Z_1)} \quad (1)$$

where V_1 and V_2 are the wind speeds measured at heights Z_1 and Z_2 , respectively.

Second, the wind shear coefficient can be considered equal to 1/7 (famously known as the 1/7th power law), as is typically and commonly assumed in the wind energy literature [14]. Then, the wind speed at a hub height can be calculated using the following equation (called the power law):

$$V_{\text{hub height}} = V_{\text{measured}} \left(\frac{Z_{\text{hub height}}}{Z_{\text{measured}}} \right)^\alpha \quad (2)$$

Third, the roughness of the site surface has an effect on the site wind speed by increasing the surface frictional stress, which consequently leads to the wind speed slowing down at the surface, affecting the vertical wind shear (wind gradient) above the surface. A roughness length is a parameter used to express the roughness of a surface. The wind speed at a hub height can be calculated when considering the roughness of

the surface by using the following equation (called the logarithmic law):

$$V_{\text{hub height}} = V_{\text{measured}} \frac{\ln(Z_{\text{hub height}}/Z_0)}{\ln(Z_{\text{measured}}/Z_0)} \quad (3)$$

where Z_0 is the roughness length [15].

In Saudi Arabia, a number of studies on wind power and resource assessments for different cities have been published. For example, Ramli *et al.* [16] used MATLAB and HOMER (Hybrid Optimization of Multiple Energy Resources) software to conduct the technical and economic analysis of a hybrid wind/solar system for the western coastal area. Their analysis showed that the share of produced electricity from solar was more than that produced by the wind, and the solar LCOE was cheaper than the wind energy. Baseer *et al.* [17] calculated the wind energy output of seven locations in Jubail using Windographer software and found that a capacity factor of 41% could be achieved. In addition, in order to decide the most suitable wind farm site, a multi-criteria decision-making (MCDM) approach, which involves considering multiple criteria to make the optimum decision, was used in Baseer *et al.* [18]. The MCDM was based on the geographic information system (GIS) modeling and found that Ras Tunara, Turaif, and Al-Wajh were the most suitable sites for wind farms. In addition, the economic feasibility of a 30 MW wind farm in Turaif, the northern region of Saudi Arabia, was studied using HOMER software [19]. It was found that an annual energy of 39,752 MWh can be generated, 1,598 tons/year of carbon emission can be avoided, and 0.0579 US\$/kWh cost of energy can be obtained. Azorin-Molina *et al.* [20] analyzed variability in and trends of observed wind speed near the surface from multiple Saudi Arabian stations for the period 1978-2013. They found a decline in wind speed of -0.058 m/s per decade over the country on an annual scale. Additionally, Alharthi *et al.* [21] evaluated the potential energy of a solar Photovoltaics-wind hybrid system for four different cities in Saudi Arabia using HOMER software. The study showed that the system was economically and environmentally feasible in Yanbu. A similar study was conducted by Shaahid [22] to assess the feasibility of an off-grid wind-diesel hybrid system for residential buildings in Yanbu using HOMER software. The study showed that the wind energy penetration for a 50 m hub height could reach 27%.

Chen *et al.* [23] quantified the potential of wind energy in Saudi Arabia in current and future climates. The study used the MENA CORDEX (Middle East North Africa Coordinated Regional Climate Downscaling Experiment) model output and found that the potential of wind energy is high in the western region of Saudi Arabia. In addition, Al-Salem *et al.* [24] studied the availability of wind power resources throughout the Arabian gulf region and found that wind power is attractive in Saudi Arabia, Qatar, and Bahrain, especially during the summer. Rehman *et al.* [25] assessed the wind power cost of 20 cities in Saudi Arabia. The study used meteorological wind data for periods between 1970 and 1982, and proposed that the maximum generated power and minimum cost were obtained in Yanbu. Similarly, Rehman [26] analyzed the wind data and wind availability at the city

of Yanbu. Meteorological wind data from the period of 1970 to 1983 was used. The analysis suggested that higher energy production and capacity factors were obtained from smaller wind machines compared to larger ones. Krishna and Al Thalhi [27] studied the potential of solar and wind energy for six regions in the Tabuk province in northwestern Saudi Arabia. The analysis showed that the coastal city of Haql, out of the six regions, had the highest potential for wind energy. Eltamaly and Farh [28] presented technical and economical assessments for five locations in Saudi Arabia using a MATLAB program that allowed them to choose the most suitable wind turbine for each location. Rafique *et al.* [29] studied the feasibility of a 100 MW grid-connected wind power plant for five cities (i.e., Dhahran, Riyadh, Jeddah, Guriat, and Najran) with different climatic conditions in Saudi Arabia. The study found that all of the cities were feasible, with Dhahran being the best. Baseer *et al.* [30] presented the characteristics of the wind speed and power of Jubail Industrial city in the eastern province of Saudi Arabia. Measured hourly mean wind speed data at three different heights (10, 50, and 90 m) was used for the period between 2008 and 2012. The annual energy production for five different commercial wind turbines was estimated and 25% was the highest capacity factor found. Moreover, the local wind shear exponent for Dhulom in Saudi Arabia was estimated by Rehman and Al-Abbadi [31] using Equation (1) for three different heights. The study also calculated the energy yield for a hypothetical 60 MW wind farm using different capacity wind turbines with different hub heights. A capacity factor of 45.56% could be achieved at Dhulom. Rehman and Al-Abbadi [13] conducted a similar study for Dhahran in Saudi Arabia, where the highest obtained capacity factor was 24%. In both studies, the authors calculated the energy yield and capacity factor using the $1/7^{\text{th}}$ wind power law, where the wind shear exponent was considered to be 0.143. More produced energy was obtained (5%–20% for Dhulom and 11%–12% for Dhahran), and higher capacity factors were achieved (1%–7.5% for Dhulom and 2%–3% for Dhahran), in both studies using the local wind shear exponent compared to the results obtained using the $1/7^{\text{th}}$ wind power law.

Compared with the above literature, this work has given more consideration to the availability of wind resources. This special consideration was done by using an updated concise weather data set and different methods of wind speed extrapolation to different heights. Moreover, to the best of our knowledge, this study is the first study to assess the feasibility and test the announced targets of a planned wind energy project. In addition, 113 commercial wind turbines with different sizes and power curves were simulated, which helped to understand the effects of these factors on the wind farm performance.

In this work, an assessment of the Dumat Al-Jandal Project was conducted. The paper is divided into different sections. Section I introduces the topic and explains the current energy situation of the electricity mix in Saudi Arabia and the motivation for utilizing renewable energy. In addition, it presents a literature review related to wind energy and its assessment in Saudi Arabia and describes the innovation of this work. A description of the project's site and data is provided in Section II, followed by a description of the

extrapolation of the wind speed to different heights in Section III. Section IV explains the economic metrics used, followed by a presentation and discussion of the results in Section V and the conclusion in Section VI.

II. SITE AND DATA DESCRIPTION

The wind power farm will be located in Dumat Al-Jandal, which is a city in the province of Al Jouf in the north of Saudi Arabia. The latitude, longitude, and the altitude of the location are 29.56° N, 40.12° E, and 562 m, respectively [25]. Wind speed, wind direction, temperature, pressure, and relative humidity were used as metrological data in this study. They were obtained from the latest updated typical metrological year (TMY3) data set, which were developed and updated by Sandia National Laboratories and the National Renewable Energy Laboratory (NREL) [32]. The TMY3 contains 8,760 weather data values, which represent every hour of a year. The TMY3 data set values are extracted from at least 10 years of data records. The TMY data sets are commonly used in designing and modeling renewable energy systems because they are concise. They represent typical metrological months and were prepared by a process of weighting several weather parameters and then concatenating the typical months' data sets to form a typical year. Therefore, the TMY data sets do not include data of extreme weather events [32]. The hourly wind speed, in the TMY data sets, was measured at an elevation of 10 m [33]. Al Jouf's TMY data set cover a period of 13 years.

One of the main obstacles to increasing wind power penetration is the intermittent nature of wind speed [34]. To obtain a good understanding of the availability of suitable wind during an entire year, the average monthly wind speed of the TMY3 data set is provided in Fig. 1. This figure shows that the average wind speed was the highest (above 4 m/s) during the months of February, April, May, and July, while the lowest values were recorded during the months of November, December, and January. In general, the average annual wind speed was about 3.7 m/s. In addition, the seasonal trend of wind speed matches with the load pattern of electricity in Saudi Arabia, where more electricity load is demanded during the summer and less is demanded during the winter [35]. Therefore, wind energy could partially replace fossil fuel-based energy.

The diurnal variation of the average wind speed is shown in Fig. 2. As shown in the figure, increasing hourly mean wind speed values were observed starting from 6:00 and peaked at 17:00. Then, decreasing hourly mean wind speed values were observed. This trend also matches the typical daily load curve in Saudi Arabia during the summer [36].

Knowing the availability of certain wind speeds in terms of the number of hours per year is important when choosing a wind turbine with the most suitable technical specifications (e.g., cut-in, cut-out, rated, survival wind speeds). Fig. 3 shows the wind duration curve of the TMY3 data set for Dumat Al-Jandal. It was generated by counting the number of hours in a year where the wind speed remained at a certain speed. The figure shows that the wind speed of 2 to 5 m/s is the most frequent, representing 68.3% of the year's hourly mean values at a 10 m height. The wind speeds of more than or equal to 3 m/s, which is the cut-in speed of most

commercial wind turbines [37], were about 66.5%.

The wind rose diagram, as shown in Fig. 4, provides information on the distribution and direction of the wind speed at a certain location. Knowing the direction of the wind speed is important when siting the wind turbines, as they should be faced toward the wind to obtain the maximum efficiency power generation [16]. It can be seen from the figure that the prevailing wind directions were north-west, east, and west, with values of 19.91%, 19.90%, and 18.69%, respectively. In addition, the wind rose diagram matched the wind duration curve in that the wind speed bins of 0–4 and 4–8 m/s were dominant.

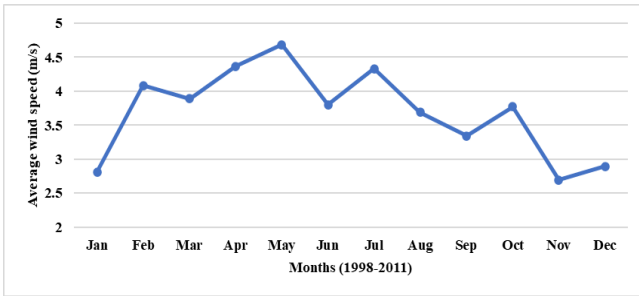


Fig. 1. The average monthly wind speed of the typical metrological year (TMY3) data set for Dumat Al-Jandal.

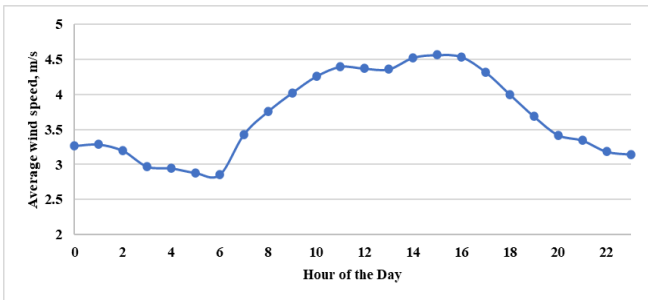


Fig. 2. The diurnal variation of the average wind speed.

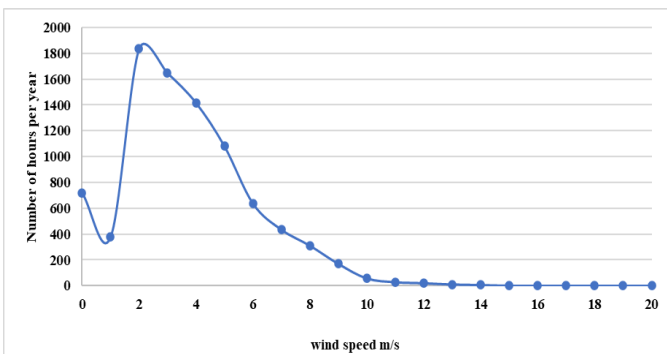


Fig. 3 Wind duration curve of the typical metrological year (TMY3) data set for Dumat Al-Jandal.

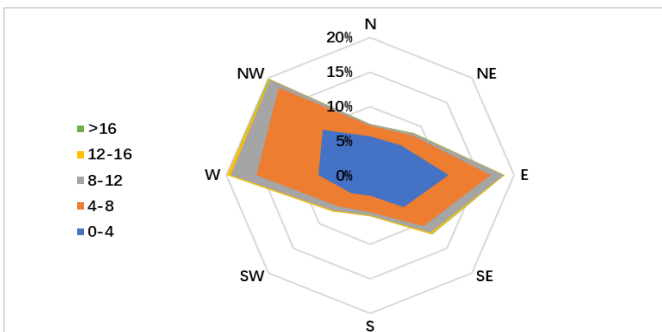


Fig. 4. Wind rose diagram for Dumat Al-Jandal.

III. EXTRAPOLATION OF WIND SPEEDS AT DIFFERENT HEIGHTS

As the hub height of the wind turbine is usually different from the height where the wind measurements are taken, the wind speeds were extrapolated to different heights. This extrapolation was done by using the previously mentioned laws for the following heights: 50 m, 80 m, 110 m, and 140 m. In general, the speed of the wind increases with height for two reasons. First, surface friction slows the wind near the earth’s surface: the rougher the surface, the more the wind slows down. Second, the air is denser near the earth’s surface, and its density decreases with height, which causes the wind to move faster. From the generated power point-of-view, the denser air is favorable as it has more molecules to hit and transmit their momentum to the blades of the wind turbine. However, the effect of wind speed on wind power generation is stronger than that of the air density. This effect is shown in the following equation:

$$P = \frac{1}{2} \rho A V^3 \quad (4)$$

where P is the power available in the wind, ρ is the air density, A is the swept area of the blades, and V is the wind speed. The swept area A is equal to πL^2 , where L is the length of the blade [38].

Extrapolation using the power law was conducted with two different wind shear coefficients. The first was the typical and commonly assumed wind shear coefficient of 1/7 [14]. The second was taken from the literature for the nearest available region that has similar terrain features, which is Arar in the north of Saudi Arabia. As taken from the literature [39], the overall mean wind shear coefficient for Arar was 0.182. In addition, to use the logarithmic law to extrapolate the wind speed at different heights, the roughness length (Z_0) is needed. As the meteorological stations in Saudi Arabia are located at airports [39], the roughness length for the airport runway areas was used, which is equal to 0.01 [40].

The frequency distributions of the wind speed values at different heights using the different laws of extrapolation were constructed and compared, as shown in Figs. 5–7. These figures are important in estimating the expected energy production from a wind turbine in conjunction with its power curve. In the figures, the hourly average wind speed over the entire period of the data was above 3 m/s (the cut-in speed of most commercial wind turbines [37]) for around 87.45% of the time for all heights (50 m, 80 m, 110 m, and 140 m) and was around 66.49% at the data collection height (10 m). By using the 1/7th power law as shown in Fig. 5, the wind speed was found to be above 6 m/s for around 46.68% of the time for all heights (50 m, 80 m, 110 m, and 140 m) and around 19.15% at the 10 m height. For above 8 m/s, the frequency of the wind speed values was around 19.15% at the 50 m and 80 m hub heights, while the share was found to be higher at the 110 m and 140 m hub heights (around 31.49%). Furthermore, the wind was found to blow above 10 m/s for around 6.91% of the time at 50 m and the percentage was higher (11.88%) at 80 m, 110 m, and 140 m. Finally, the wind speed values were above 12 m/s for around 3.36% of the time at heights of 50 m and 80 m, and for around 6.91% of the time at heights of 110 m and 140 m.

By using the power law with the shear coefficient equal to 0.182, as shown in Fig. 6, the wind speed was found to be above 6 m/s for around 46.68% of the time for all hub heights (50 m, 80 m, 110 m, and 140 m). For above 8 m/s, the frequency of wind speed values was around 19.15% at 50 m, while the share was found to be higher at 80 m, 110 m, and 140 m (around 31.49%). Additionally, the wind was found to blow above 10 m/s for around 11.88% of the time at 50 m and 80 m, and the percentage was higher (19.15%) at 110 m and 140 m. Finally, the wind speed values were above 12 m/s for around 3.36% of the time at the height of 50 m, and around 6.91% of the time at 80 m, 110 m, and 140 m.

By using the logarithmic law, as shown in Fig. 7, the wind

speed was found to be above 6 m/s for around 31.49% of the time for 50 m, while it reached around 47.68% for the other heights (80 m, 110 m and 140 m). For above 8 m/s, the frequency of the wind speed values was around 19.15% at all heights (50 m, 80 m, 110 m, and 140 m). Furthermore, the wind was found to blow above 10 m/s for around 6.91% of the time at 50 m, and the percentage was higher (11.88%) at 80 m, 110 m, and 140 m. The wind speed values were above 12 m/s for around 3.36% of the time at the heights 50 m, 80 m, and 110 m, and for around 6.91% of the time at 140 m. The frequency distribution figures make the differences seem small, but for the produced power and efficiency of the wind turbines, these differences are important, as will be shown in the results section.

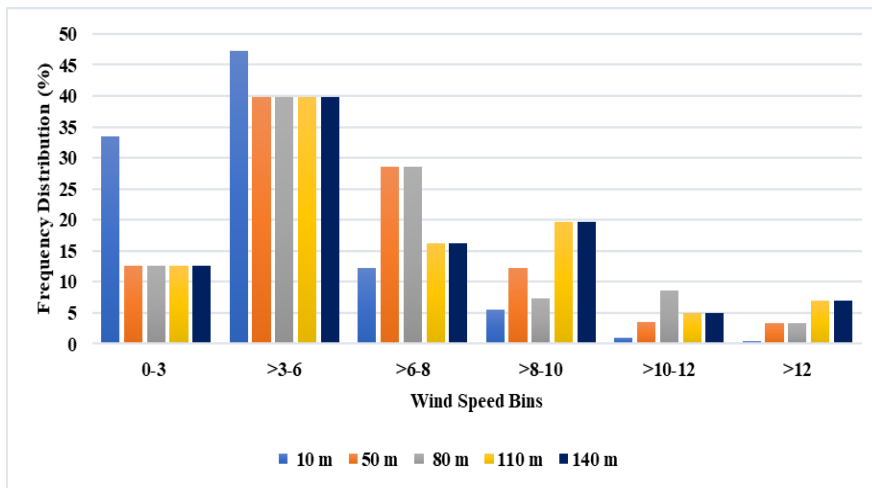


Fig. 5. Comparison of the frequency distribution at different hub heights using the 1/7th power law.

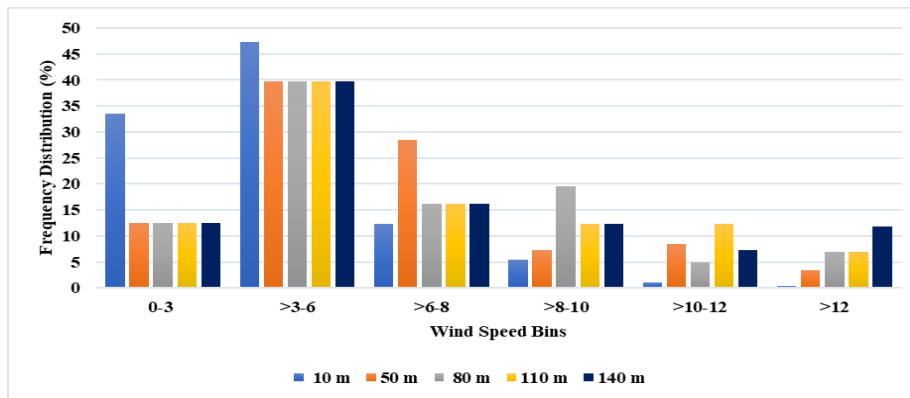


Fig. 6. Comparison of the frequency distribution at different hub heights using the power law with α equals 0.182.

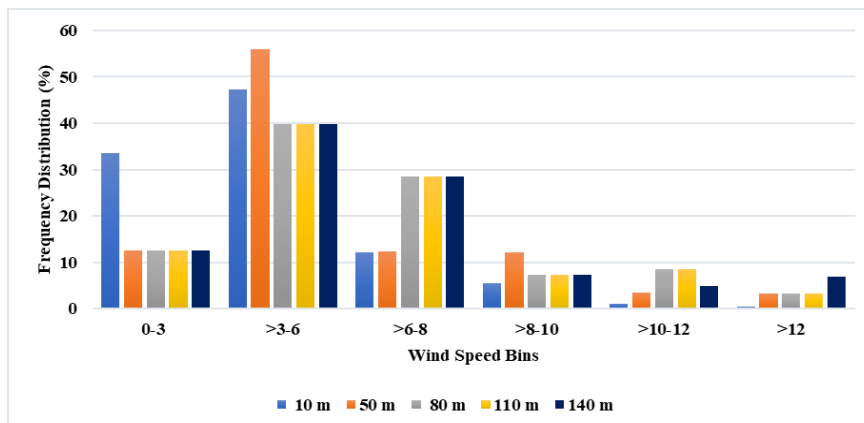


Fig. 7. Comparison of the frequency distribution at different hub heights using the logarithmic law.

IV. ECONOMIC ANALYSIS

The economic metrics of the LCOE and net present value (NPV) were calculated and used in this study. The LCOE is a measure of the average lifetime costs of the produced power. It is usually used for a comparison of electricity technologies or systems. The mathematical formula employed to calculate LCOE is as follows:

$$LCOE = \frac{FCR \times TCC + FOC}{AEP} + VOC \quad (5)$$

where FCR is the fixed charge rate (\$), TCC is the capital cost (\$), FOC is the fixed annual operating cost (\$), AEP is the annual electricity production (kWh), and VOC is the variable operating cost (\$/kwh). The NPV is the sum of all future cash flows in today’s money minus the initial investment. It measures the attractiveness of an investment, where a positive NPV indicates an economically feasible project, while a negative NPV indicates the opposite. The mathematical formula used to calculate the NPV is as follows:

$$NPV = \sum_{n=0}^N \frac{C_n}{(1+d)^n} \quad (6)$$

where C_n is the cash flow in year n, d is the discounted rate, and N is the analysis period in years [41]. The financial parameters of the inflation rate, discounted rate, debt interest rate, debt ratio, debt term, and project life for Saudi Arabia were taken from the literature [29] and are shown in Table III.

TABLE III: THE FINANCIAL PARAMETERS USED

Parameter	Value
Inflation Rate	3%
Discounted Rate	0%
Debt Interest Rate	0%
Debt Ratio	25%
Debt Term	20 years
Project Life	25 years

V. SIMULATION RESULTS AND DISCUSSION

The Dumat Al-Jundal wind farm was simulated using the System Advisor Model (SAM) software. The National Renewable Energy Laboratory (NREL) developed the SAM with funds received from the U.S. Department of Energy [41]. The simulations were done using different hub heights with the three previously mentioned extrapolation methods. These simulations were performed for 113 commercial wind turbines with different sizes and power curves (their technical data is shown in Appendix A.1). This detailed analysis helps to understand the effects of these factors on the performance of the wind farm technically and economically. The technical side was determined by calculating the total energy output and capacity factor, while the economic side was determined by calculating the LCOE and NPV. The capacity factor of the plant was obtained by dividing the total actual generated output by its potential energy output if the full nameplate capacity could be achieved. The most and least efficient wind machine types for each extrapolation method are shown in Table IV. Table IV shows the technical and economic performances of the most and least efficient wind machine types for the 400 MW Dumat Al-Jandal wind farm project. The wind power curves for these wind machines are depicted in Figs. 8, 9. For the extrapolation using the logarithmic law, the highest capacity factor was 26.8% (939,913,856 kWh) using the 2 MW Gamesa G114 wind turbine at an elevation of 140 m, while the lowest capacity factor was 7.4% (939,913,856 kWh) using the 1650 KW Vestas V-66 wind turbine at an elevation of 50 m. In addition, the lowest LCOE price was 4.75 ¢/kWh, which was possible to achieve with the 2 MW Gamesa G114 wind turbine at an elevation of 140 m, while the highest LCOE price was 18.62 ¢/kWh with the 1650 KW Vestas V-66 wind turbine at an elevation of 50 m.

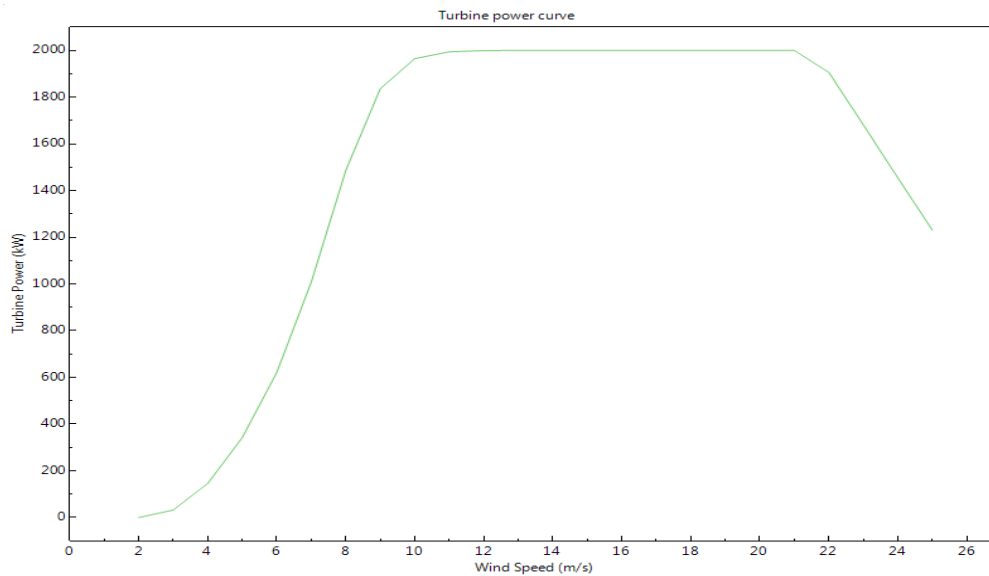


Fig. 8. Wind power curve for the 2 MW Gamesa G114 wind machine [42].

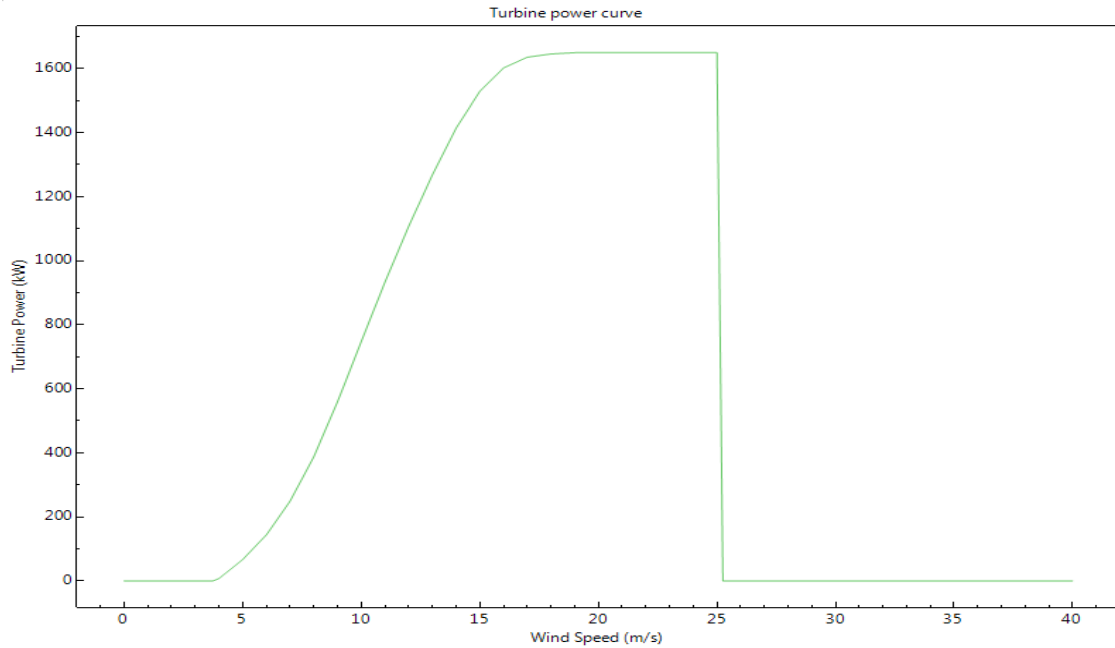


Fig. 9. Wind power curve for the 1650 KW Vestas V-66 wind machine [42].

TABLE IV: THE TECHNICAL AND ECONOMIC PERFORMANCE OF THE MOST AND LEAST EFFICIENT WIND MACHINE TYPES FOR THE 400 MW DUMAT AL-JANDAL WIND FARM PROJECT

Hub Height	Metric	Logarithmic Law		1/7th Power Law		Power Paw with $\alpha=0.182$	
		Highest	Lowest	Highest	Lowest	Highest	Lowest
		Gamesa G114 2MW	Vestas V66-1650 KW	Gamesa G114 2MW	Vestas V66-1650 KW	Gamesa G114 2MW	Vestas V66-1650 KW
50	Annual energy (kWh)		260,748,391		272,007,680		327,870,304
	Capacity factor	too low Height	7.40%	too low Height	7.80%	too low Height	9.40%
	LCOE (¢/kWh)		18.62		17.8		14.56
	Net present value		\$552,723,911		\$550,781,568		\$538,387,072
80	Annual energy (kWh)	830,799,488	305,608,249	895,628,416	332,127,904	1,041,003,328	417,476,128
	Capacity factor	23.70%	8.70%	25.60%	9.50%	29.70%	11.90%
	LCOE (¢/kWh)	5.28	15.77	4.83	14.43	4.02	11.25
	Net present value	\$486,956,096	\$547,518,151	\$478,974,848	\$543,804,992	\$456,182,560	\$527,988,832
110	Annual energy (kWh)	894,268,032	338,518,471	976,744,832	378,194,176	1,153,692,032	486,558,592
	Capacity factor	25.50%	9.70%	27.90%	10.80%	32.90%	13.90%
	LCOE (¢/kWh)	4.84	14.15	4.36	12.57	3.55	9.54
	Net present value	\$479,590,912	\$543,699,129	\$469,561,728	\$538,459,200	\$443,859,776	\$519,972,160
140	Annual energy (kWh)	939,913,856	364,091,236	1,039,009,152	416,259,360	1,243,976,704	543,217,152
	Capacity factor	26.80%	10.40%	29.70%	11.90%	35.50%	15.50%
	LCOE (¢/kWh)	4.57	13.1	4.05	11.34	3.23	8.45
	Net present value	\$474,293,984	\$540,731,520	\$462,336,288	\$534,041,952	\$432,628,576	\$513,397,248

For the extrapolation using the 1/7th power law, the highest capacity factor was 29.7% (1,039,009,152 kWh) using the 2 MW Gamesa G114 wind turbine at an elevation of 140 m, while the lowest capacity factor was 7.8% (272,007,680 kWh) using the 1650 KW Vestas V-66 wind turbine at an elevation of 50 m. In addition, the lowest LCOE price was 4.05 ¢/kWh, which was possible to achieve with the 2 MW Gamesa G114 wind turbine at an elevation of 140 m, while the highest LCOE price was 17.8 ¢/kWh with the 1650 KW Vestas V-66 wind turbine at an elevation of 50 m.

For the extrapolation using the power law with $\alpha = 0.182$, the highest capacity factor was 35.5% (1,243,976,704 kWh)

using the 2 MW Gamesa G114 wind turbine at an elevation of 140 m, while the lowest capacity factor was 9.4% (327,870,304 kWh) using the 1650 KW Vestas V-66 wind turbine at an elevation of 50 m. In addition, the lowest LCOE price was 3.23 ¢/kWh, which was possible to achieve with the 2 MW Gamesa G114 wind turbine at an elevation of 140 m, while the highest LCOE price was 14.56 ¢/kWh with the 1650 KW Vestas V-66 wind turbine at an elevation of 50 m. For the 2 MW Gamesa G114 wind turbine at a hub height of 50 m, the “too low height” occurred because the turbine’s rotor diameter (114 m) was too high for that elevation.

Regarding the NPV, the Dumat Al-Jandal project was

economically feasible and attractive with all types of wind machines. As in Table V, the analysis shows the effect of the increase in height on all the studied metrics for the most efficient wind turbine (the 2 MW Gamesa G114 wind turbine). For the height change from 80 m to 110 m and 110 m to 140 m using the logarithmic law, the results demonstrated a 7.64% and 5.10% higher energy output, 7.59% and 5.10% higher capacity factor, 8.33% and 5.58% lower LCOE, and 1.51% and 1.1% lower NPV, respectively. For the height change from 80 m to 110 m and 110 m to 140

m using the 1/7th power law, the results revealed a 9.06% and 6.37% higher energy output, 8.98% and 6.45% higher capacity factor, 9.73% and 7.11% lower LCOE, and 1.97% and 1.54% lower NPV, respectively. For the height change from 80 m to 110 m and 110 m to 140 m using the power law with $\alpha = 0.182$, the data showed a 10.83% and 7.83% higher energy output, 10.77% and 7.90% higher capacity factor, 11.69% and 9.01% lower LCOE, and 2.70% and 2.53% lower NPV, respectively.

TABLE V: PERCENT INCREASE IN ALL METRICS WITH AN INCREASE IN HUB HEIGHT FOR THE MOST EFFICIENT WIND TURBINE (THE 2 MW GAMESA G114 WIND TURBINE)

Hub Height's Increase	Metric	Logarithmic Law	1/7th Power Law	Power Law with $\alpha=0.182$
80-110	Annual energy	7.64	9.06	10.83
	Capacity factor	7.59	8.98	10.77
	LCOE	-8.33	-9.73	-11.69
	Net present value	-1.51	-1.97	-2.70
110-140	Annual energy	5.10	6.37	7.83
	Capacity factor	5.10	6.45	7.90
	LCOE	-5.58	-7.11	-9.01
	Net present value	-1.10	-1.54	-7.87

VI. CONCLUSION

The feasibility of the 400 MW Dumat Al-Jandal wind farm project, which is the first utility-scale wind farm in Saudi Arabia, was simulated and examined in this study using the SAM software. The ability of assessing the availability of wind resources is a crucial factor in developing a new wind energy project. For this reason, the latest updated typical metrological year (TMY3) data set was used for the wind resources. The TMY3 data set showed that the average wind speed was the highest (above 4 m/s) during the months of February, April, May, and July, while the lowest values were recorded during the months of November, December, and January. This pattern of wind speed matches the load pattern of electricity in Saudi Arabia, where a greater electricity load is demanded during the summer. As the hub height of the wind turbine is usually different from the height at which the wind measurements are taken, the wind speeds were extrapolated to different heights. Therefore, the TMY3 data was extrapolated to different heights using different methods. These methods are the power law using two different shear coefficients and the logarithmic law. The simulations were performed for 113 commercial wind turbines with different sizes and power curves in order to enhance our understanding of the effects of these factors on the performance of the wind farm, both technically and economically. The technical analysis showed that the capacity factors of the most efficient wind machine type varied from 35.5%–26.8%, 32.9%–25.5%, and 29.7%–23.7% for the heights 140 m, 110 m, and 80 m, respectively. From an economic perspective, the LCOE of the most efficient wind machine type varied from 3.23–4.57, 3.55–4.84, and 4.02–5.82 ¢/kWh for the heights 140 m, 110 m, and 80 m, respectively. The lowest possible LCOE (3.23 ¢/kWh) according to this analysis is in the same range

of the submitted LCOE by the winning bidder [11]. The NPV showed that the Dumat Al-Jandal project was both economically feasible and attractive. Finally, a large variation existed in the technical and economical results of the analysis using different extrapolation methods. This large variation showed the importance of investing in precise on-site wind speed measurements, which will reduce the risk of investing in the wrong project. Future work will include comparing SAM's predictions with the actual data of the plant after its commission in the near future.

APPENDIX

TABLE A.I: THE TECHNICAL DATA OF THE 113 WIND MACHINES USED IN THIS ANALYSIS

Wind Turbine	Cut-in speed (m/s)	Cut-out speed (m/s)	Rated speed (m/s)	Rated output (kW)	Rotor diameter (m)
Enercon E40	3	25	14	500	40
EWT directwind 52 500 kw	3	25	10	500	52
EWT directwind 54 500 kw	3	25	11	500	54
Powerwind 56-500	4	25	10	500	56
Vestas V39-500KW	5	25	15	500	39
Nordex N43-600	3	25	15.5	600	43
Suzlon S52 600	4	25	13	600	52
Tacke T600-48	4	20	---	600	48
Tacke TW-600-46	3	25	21	600	46
Vestas V42-600	5	25	17	600	42
Vestas V44-600	5	20	17	600	44
Vestas V47-600	5	25	17	600	47
NEG Micon multi-power 44-750	4	25	---	750	44
NEG Micon multi-power 48-750	4	25	---	750	48
WindEnergyLebanon 750kw 54m	4	25	13	750	54
WindEnergyLebanon 750kw 57m	4	25	12	750	57

Zond Z-50 750	4	25	12.25	750	50	Siemens SWT 2.3 MW-108m	3	20	11	2300	108
Gamesa G52 850	4	25	16	850	52	Mitsubishi MWT 92-2.4	3	25	12.25	2400	92
Gamesa G58 850	3	21	16	850	58	Mitsubishi MWT 95-2.4	3	25	12.5	2400	95
Vestas V52-850	4	25	16	850	52	Fuhrlander FL 2500-100	3.5	25	11.5	2500	100
Amercas wind energy 52-900	2	25	15	900	52	Fuhrlander FL 2500-80	4	25	14	2500	80
Amercas wind energy 54-900	2	25	14	900	54	Fuhrlander FL 2500-90	4	25	12.75	2500	90
NEG Micon 52-900	3.5	25	---	900	52	GE 2.5XL	3.5	25	12.5	2500	100
Mitsubishi MWT 1000	4	25	13.5	1000	57	Liberty C89	4	25	14.5	2500	89
Mitsubishi MWT 1000A	3	25	12.5	1000	61.4	Liberty C93	4	25	14	2500	93
Vergent GEV HP-62M-1000	3	25	15	1000	62	Liberty C96	4	25	13.75	2500	96
Suzlon S64-1250	3.5	25	14	1250	64	Liberty C99	4	25	13.25	2500	99
Suzlon S66-1250	3	25	14	1250	66	Liberty Clipper C100	4	25	14	2500	100
Bonus 1300	4	25	17	1300	62	Nordex N100-2500	3.25	25	13	2500	100
Nordex N60-1300	3.25	25	---	1300	60	Nordex N80-2500	3.25	25	15	2500	80
AAER A-1500-70	3.25	25	12	1500	70	Nordex N90-2500	3.5	25	13	2500	90
AAER A-1500-77	3.25	25	12	1500	77	Vensys 100-2500	4	25	14	2500	100
Composite IEC Class I	4	25	17.25	1500	90	Vensys 109-2500	4	25	13	2500	109
Composite IEC Class II	4	25	15	1500	90	Vensys 112-2500	4	25	12	2500	112
Composite IEC Class III	3	22	15	1500	90	Leitwind LTW101m 3MW	3	25	12	3000	101
Fuhrlander FL 1500 70	3	25	12	1500	70	Siemens SWT 3 MW-101m	3	25	14	3000	101
Fuhrlander FL 1500 77	3	25	11	1500	77	Senvion 3MW 122m	4	25	12	3000	122
GE 1.5 XLE	3.5	20	11	1500	82.5	Vestas V112-3.0	3	25	11.75	3000	112
GE 1.5s	4	25	13.5	1500	70	Vestas V90-3.0	3.5	25	15	3000	90
GE 1.5sle	3.5	25	14	1500	77	Senvion 3.2MW 114m	4	25	12	3200	114
Leitwind LTW77m	4	25	12	1500	77	RePower 3XM	3.5	25	12.5	3300	104
Leitwind LTW80m	4	25	12	1500	80	Senvion 3.4 MW 114m	4	25	14	3400	114
NEG Micon 72-1500	5	25	15	1500	72	General Electric GE 3.6sl 111m	4	27	15	3600	111
Nordex N70-1500	4	25	13	1500	70	Siemens 3.6 MW-120m	4	25	15	3600	120
Nordex S77-1500	4	25	13	1500	77	Siemens SWT 3.6 MW-107m	4	25	15	3600	107
Suzlon S82-1.5	4	20	14	1500	82	Gamesa G128 4.5MW	4	27	13	4500	128
Vensys 70-1500	4	25	15	1500	70	Areva Multibird m5000	3.75	25	12.5	5000	116
Vensys 77-1500	4	22	14	1500	77	BARD 5	3.25	25	12.5	5000	122
Vensys 82-1500	4	22	13	1500	82	RePower 5M	3.75	25	13.25	5000	126
NEG Micon 82-1650	4	20	14	1650	82	Enercon E126 127m 7500kw	3	25	16	7500	127
Vestas V66-1650	4	25	19	1650	66	Vestas 164 8mw	4	25	13	8000	164
Vestas V82-1650	3.5	20	13.5	1650	82						
Leitwind LTW80 1.8MW	4	25	12	1800	80						
Vestas V100-1.8	4	20	11.5	1800	100						
Vestas V80-1.8	4	25	14	1800	80						
Vestas V90-1.8	3.5	25	11.75	1800	90						
DeWind D8(8.2)	3	25	13.25	2000	80						
EWT directwind 90 m 2mw	4	25	13	2000	90						
EWT directwind 96m 2mw	4	25	11	2000	96						
Gamesa G80 2MW	4	25	17	2000	80						
Gamesa G83 2MW	4	25	17	2000	83						
Gamesa G87 2MW	4	25	17	2000	87						
Gamesa G90 2MW	3	21	17	2000	90						
Gamesa G97 2MW	3	25	14	2000	97						
Gamesa G114 2MW	3	25	13	2000	114						
Leitwind LTW70 2MW	4	25	14	2000	70						
NREL 2000KW	3	25	10	2000	55						
Vestas V80-2.0	4	25	16	2000	80						
Vestas V90-2.0	2.5	25	12.75	2000	90						
Vestas V100-2.0	3	22	12	2000	100						
Vestas V110-2.0	3	20	15	2000	110						
Enercon E82 2050kw	2	25	13	2050	82						
RePower MM82	3.5	25	14.5	2050	82						
RePower MM92	3	24	12.5	2050	92						
Suzlon S88	4	25	14	2100	88						
Nordex N90-2300	3.25	25	13	2300	90						
Siemens SWT 2.3 MW-93	3.5	25	13.5	2300	93						
Siemens SWT 2.3 MW-101m	4	25	12	2300	101						

CONFLICT OF INTEREST

The authors declare that they have no conflict of interest.

AUTHOR CONTRIBUTIONS

Kamel and Ramzi carried out the research, wrote and revised the article. Kamel conceptualised the central research idea and provided the theoretical framework. Kamel and Ramzi designed the research, supervised research progress; Ramzi anchored the review, revisions and approved the article submission.

ACKNOWLEDGMENT

This study was supported by the Ministry of Education in Saudi Arabia through Taibah University. Any opinions, findings, recommendations, and conclusions expressed herein are those of the authors and are not necessarily those of the Ministry of Education.

REFERENCES

- [1] OPEC, Asb_2018. (2018). [Online]. 26. Available: https://www.opec.org/opec_web/en/data_graphs/330.htm%0Ahttps://www.opec.org/opec_web/en/publications/202.htm
- [2] Government of Saudi Arabia, Saudi Arabia Vision 2030. (2016). [Online]. 85. Available: http://vision2030.gov.sa/sites/default/files/report/Saudi_Vision2030_EN_2017.pdf
- [3] The Electricity & Cogeneration Regulatory Authority (ECRA), annual statistical booklet for electricity and seawater desalination industries. (2019). [Online]. Available: https://ecra.gov.sa/en-us/MediaCenter/DocLib2/Lists/SubCategory_Library/ecra%20sat_book_16.pdf
- [4] M. M. Damoom, S. Hashim, M. S. Aljohani, and M. A. Saleh, "Adding sustainable sources to the Saudi Arabian electricity sector," *Electr. J.*, vol. 31, pp. 20–28, 2018.
- [5] K. Almutairi, G. Thoma, and A. Durand-Morat, "Ex-ante analysis of economic, social and environmental impacts of large-scale renewable and nuclear energy targets for global electricity generation by 2030," *Sustain.*, vol. 10, 2018.
- [6] K. Almutairi, G. Thoma, J. Burek, S. Algarni, and D. Nutter, "Life cycle assessment and economic analysis of residential air conditioning in Saudi Arabia," *Energy Build.*, vol. 102, pp. 370–379, 2015.
- [7] Global Carbon Atlas. (2019). [Online]. Available: <http://www.globalcarbonatlas.org/en/content/welcome-carbon-atlas>
- [8] M. Groissböck and M. J. Pickl, "Fuel-price reform to achieve climate and energy policy goals in Saudi Arabia: A multiple-scenario analysis, Util.," *Policy*, vol. 50, 2018.
- [9] Investsaudi, *Renewable Energy*, 2019. doi:10.1016/B978-1-85617-804-4.00005-7.
- [10] NATIONAL RENEWABLE ENERGY PROGRAM. (2018). [Online]. Available: <https://ksa-climate.com/making-a-difference/nrep/>
- [11] (MEIM) the Renewable Energy Project Development Office (REPDO) at the Ministry of Energy, Overview of Saudi Arabia's Renewable Energy Program, 2019.
- [12] Masdar, Dumat Al Jandal Project. (October 16, 2021). [Online]. Available: <https://masdar.ae/en/masdar-clean-energy/projects/dumat-al-jandal>
- [13] S. Rehman and N. M. Al-Abbadi, "Wind shear coefficients and energy yield for Dhahran, Saudi Arabia," *Renew. Energy*, vol. 32, pp. 738–749, 2007.
- [14] B. Storm, J. Dudhia, S. Basu, A. Swift, and I. Giammanco, "Evaluation of the weather research and forecasting model on forecasting low-level jets: Implications for wind energy," *Wind Energy*, vol. 12, pp. 81–90, 2009.
- [15] M. Ragheb. Wind shear, roughness classes and turbine, production. (2015). [Online]. Available: http://mragheb.com/NPRE_475_Wind_Power_Systems/Wind_Shear_Roughness_Classes_and_Turbine_Energy_Production.pdf
- [16] M. Ramli, A. Hiendro, and Y. Al-Turki, "Techno-economic energy analysis of wind/solar hybrid system: Case study for western coastal area of Saudi Arabia," *Renew. Energy*, vol. 91, pp. 374–385, 2016.
- [17] M. A. Baseer, J. P. Meyer, S. Rehman, and M. Alam, "Wind power characteristics of seven data collection sites in Jubail, Saudi Arabia using Weibull parameters," *Renew. Energy*, pp. 1–30, 2017.
- [18] M. A. Baseer, S. Rehman, J. P. Meyer, and M. Alam, "GIS-based site suitability analysis for wind farm development in Saudi Arabia," *Energy*, 2017.
- [19] S. M. Shaahid, L. M. Alhems, and M. K. Rahman, "Potential of development of wind farms in Turaif Saudi Arabia – A case study to mitigate the challenges of fossil fuel depletion," *International Journal of Applied Engineering Research*, vol. 13, pp. 1798–1804, 2018.
- [20] C. Azorin-molina, S. Rehman, J. A. Guijarro, T. R. Mcvican, L. Minola, and S. M. Vicente-serrano, "Recent trends in wind speed across Saudi Arabia, 1978 – 2013: A break in the stilling," *International Journal of Climatology*, vol. 38, pp. 966–984, 2018.
- [21] Y. Z. Alharthi, M. K. Siddiki, and G. M. Chaudhry, "Resource assessment and techno-economic analysis of a grid-connected solar PV-wind hybrid system for different locations in Saudi Arabia," *Sustainability*, 2018.
- [22] S. M. Shaahid, "Techno-economics of off-grid hybrid wind-diesel power systems for electrification of residential buildings of Yanbu – A potential industrial location of Saudi Arabia," *International Journal of Global Warming*, vol. 16, pp. 86–101, 2018.
- [23] G. Marc, W. Chen, S. Castruccio, G. Mg, C. P. Current, W. Chen, and S. Castruccio, "Current and future estimates of wind energy potential over Saudi Arabia over Saudi Arabia," *JGR: Atmospheres*, 2018.
- [24] K. Al-salem, S. Neelamani, and W. Al-nassar, "Wind energy map of Arabian gulf," *Natural Resources*, pp. 212–228, 2018.
- [25] S. Rehman, T. O. Halawani, and M. Mohandes, "Wind power cost assessment at twenty locations in the Kingdom of Saudi Arabia," *Renew. Energy*, vol. 28, 2003.
- [26] S. Rehman, "Wind energy resources assessment for Yanbo, Saudi Arabia," *Energy Convers. Manag.*, vol. 45, pp. 2019–2032, 2004.
- [27] F. A. A. Thalhi and L. V. Krishna, "Solar and wind energy potential in the Tabuk region, Saudi Arabia," *Int. J. Appl. Sci. Technol.*, vol. 5, pp. 12–22, 2015.
- [28] A. M. Eltamaly and H. M. Farh, "Wind energy assessment for five locations in Saudi Arabia," *J. Renew. Sustain. Energy.*, vol. 4, 2012.
- [29] M. M. Rafique, S. Rehman, M. M. Alam, and L. M. Alhems, "Feasibility of a 100 MW installed capacity wind farm for different climatic conditions," *Energies*, vol. 11, 2018.
- [30] M. A. Baseer, J. P. Meyer, M. M. Alam, and S. Rehman, "Wind speed and power characteristics for Jubail industrial city, Saudi Arabia," *Renew. Sustain. Energy Rev.*, vol. 52, pp. 1193–1204, 2015.
- [31] S. Rehman and N. M. Al-Abbadi, "Wind shear coefficient, turbulence intensity and wind power potential assessment for Dhulom, Saudi Arabia," *Renew. Energy.*, vol. 33, pp. 2653–2660, 2008.
- [32] D. S. Renné, "Resource assessment and site selection for solar heating and cooling systems," *Elsevier Ltd*, 2016.
- [33] S. M. S. Sadati, E. Jahani, O. Taylan, and D. K. Baker, "Sizing of photovoltaic-wind-battery hybrid system for a mediterranean island community based on estimated and measured meteorological data," *J. Sol. Energy Eng.*, vol. 140, 2017.
- [34] G. Ren, J. Liu, J. Wan, Y. Guo, and D. Yu, "Overview of wind power intermittency: Impacts, measurements, and mitigation solutions," *Appl. Energy*, vol. 204, pp. 47–65, 2017.
- [35] Electricity & Cogeneration Regulatory Authority, Statistical Booklet. (2018). [Online]. Available: <http://www.ecra.gov.sa/en-us/dataandstatistics/pages/DataAndStatistics>
- [36] A. Jubran and B. Peter, "Reducing high energy demand associated with air-conditioning needs in Saudi Arabia," *Energies*, vol. 12, pp. 1–15, 2019.
- [37] B. S. Pali and S. Vadhera, "A novel pumped hydro-energy storage scheme with wind energy for power generation at constant voltage in rural areas," *Renew. Energy*, vol. 127, pp. 802–810, 2018.
- [38] U. Ahrens, M. Diehl, and R. Schmehl, *Airborne Wind Energy*, 2013.
- [39] S. Rehman, *Wind Power Resource Assessment, Design of Grid-Connected Wind Farm and Hybrid Power System Wind Power Resource Assessment, Design of Grid-Connected Wind Farm and Hybrid Power System*, 2012.
- [40] M. H. Zhang, *Wind Resource Assessment and Micro-siting: Science and Engineering*, John Wiley & Sons, 2015.
- [41] NREL System Advisor Model (SAM), SAM's Help system. (2019). [Online]. Available: https://sam.nrel.gov/images/web_page_files/sam-help-2018-11-11-r4.pdf
- [42] National Renewable Energy Laboratory, System Advisor Model Software, 2013.

Copyright © 2022 by the authors. This is an open access article distributed under the Creative Commons Attribution License which permits unrestricted use, distribution, and reproduction in any medium, provided the original work is properly cited ([CC BY 4.0](https://creativecommons.org/licenses/by/4.0/)).

Kamel Almutairi is an assistant professor of chemical engineering at Taibah University, Madinah, Saudi Arabia. He received his B.S. in 2007 in chemical engineering from King Fahd University of Petroleum and Minerals, Saudi Arabia. He received his M.S. degree in 2012 in chemical engineering from Oklahoma State University. In 2018, Almutairi obtained his Ph.D. degree in chemical engineering from University of Arkansas.

Ramzi Alahmadi is an assistant professor of industrial engineering at Taibah University, Madinah, Saudi Arabia. He received his B.S. in 2010 in mechanical engineering from Taibah University, Saudi Arabia. He received his M.S. degree in 2013 in industrial engineering from University of Pittsburgh. In 2017, Alahmadi obtained his Ph.D. degree in industrial engineering from Texas Tech University.